Microscopy Microanalysis

Original Article

Assessing Soft-Tissue Shrinkage Estimates in Museum Specimens Imaged With Diffusible Iodine-Based Contrast-Enhanced Computed Tomography (diceCT)

Brandon P. Hedrick¹, Laurel Yohe², Abby Vander Linden³, Liliana M. Dávalos², Karen Sears⁴, Alexa Sadier⁴, Stephen J. Rossiter⁵, Kalina T. J. Davies⁵ and Elizabeth Dumont⁶

¹Department of Organismic and Evolutionary Biology, Harvard University, Cambridge, MA 02138, USA, ²Department of Ecology and Evolution, Stony Brook University, 650 Life Sciences Building, Stony Brook, NY 11794, USA, ³Graduate Program in Organismic and Evolutionary Biology, University of Massachusetts Amherst, Amherst, MA 01003, USA, ⁴Department of Animal Biology, University of Illinois at Urbana-Champaign, Urbana, IL 61801, USA, ⁵School of Biological and Chemical Sciences, Queen Mary University of London, London E1 4NS, UK and ⁶School of Natural Sciences, University of California-Merced, Merced, CA 95343, USA

Abstract

The increased accessibility of soft-tissue data through diffusible iodine-based contrast-enhanced computed tomography (diceCT) enables comparative biologists to increase the taxonomic breadth of their studies with museum specimens. However, it is still unclear how soft-tissue measurements from preserved specimens reflect values from freshly collected specimens and whether diceCT preparation may affect these measurements. Here, we document and evaluate the accuracy of diceCT in museum specimens based on the soft-tissue reconstructions of brains and eyes of five bats. Based on proxies, both brains and eyes were roughly 60% of the estimated original sizes when first imaged. However, these structures did not further shrink significantly over a 4-week staining interval, and 1 week in 2.5% iodinebased solution yielded sufficient contrast for differentiating among soft-tissues. Compared to six "fresh" bat specimens imaged shortly after field collection (not fixed in ethanol), the museum specimens had significantly lower relative volumes of the eyes and brains. Variation in field preparation techniques and conditions, and long-term storage in ethanol may be the primary causes of shrinkage in museum specimens rather than diceCT staining methodology. Identifying reliable tissue-specific correction factors to adjust for the shrinkage now documented in museum specimens requires future work with larger samples.

Key words: iodine-staining, microCT, bats, shrinkage, diceCT

(Received 27 October 2017; revised 9 February 2018; accepted 29 April 2018)

Introduction

The increased availability and lower cost of non-invasive imaging has led many comparative morphologists back to museum collections in order to obtain broad taxonomic samples for use in developmental and evolutionary analyses. Micro-computed tomography (μ CT) is now a relatively inexpensive method for capturing the three-dimensional (3D) geometry of bone and is commonly used in comparative studies. Unlike bone, soft-tissue has low X-ray attenuation and so requires the extra step of staining to enhance contrast before µCT scanning. Metscher (2009a, 2009b) developed a method of increasing contrast by exposing specimens to an iodine-based solution (I2KI), a technique known as diffusible iodine-based contrast-enhanced computed tomography (diceCT). Although relatively new, diceCT has already been used on a wide variety of organisms

Author for correspondence: Brandon P. Hedrick, E-mail: bphedrick1@gmail.com Sadier A, Rossiter SJ, Davies KTJ, Dumont E (2018) Assessing Soft-Tissue Shrinkage Estimates in Museum Specimens Imaged With Diffusible Iodine-Based Contrast-Enhanced Computed Tomography (diceCT). Microsc Microanal. doi: 10.1017/S14319276

Cite this article: Hedrick BP, Yohe L, Vander Linden A, Dávalos LM, Sears K,

including, among others, invertebrates (Metscher, 2009b), alligators (Tsai & Holliday, 2011; George & Holliday, 2013), quail (Tahara & Larsson, 2013), starlings (Gold et al., 2016), bats (Herdina et al., 2010), dogs (Aslanidi et al., 2012; 2013), and rodents (Jeffery et al., 2011; Stephenson et al., 2012).

In comparison with other visualization methods such as histology and other staining methods, diceCT offers several advantages: visualization of soft-tissue at high resolution, versatility in staining different kinds of tissues, and time efficiency. Efforts to visualize soft-tissue structures have been ongoing for decades and have been dominated by time-consuming, destructive histological techniques (Shenkar et al., 2008; Herdina et al., 2010; Chandler et al., 2011; Aslanidi et al., 2013; Descamps et al., 2014; Gignac et al., 2016). Compared to histology, diceCT is reversible and thus does not require destroying unique and valuable museum specimens (Gignac & Kley, 2014; Gignac et al., 2016). In addition to being non-destructive and relatively fast, in some cases it has been shown that diceCT has the potential to be more effective than histology for the visualization of small soft-tissue structures (e.g., Girard et al. 2016). In addition to histology and before the widespread use of diceCT, osmium tetraoxide-based staining was often used to enhance contrast for μ CT studies

(Descamps et al., 2014). It has been shown to be especially successful for staining specimens smaller than 2 mm in diameter (Tessler et al., 2016). DiceCT is an improvement for larger specimens because it is less toxic and works better with specimens that have been stored in ethanol, as have most museum specimens (Metscher, 2009a, 2009b; Descamps et al., 2014). Pauwels et al. (2013) performed an exploratory analysis on a wide variety of potential staining methods and found that I_2KI was one of the most effective methods of staining soft-tissues for high-resolution visualization.

Although diceCT is becoming a standard for non-destructive visualization of soft-tissue, it is not without problems. Since its inception, shrinkage was noted in specimens stained with I2KI (Metscher, 2009a), with tissues such as brains and eyes being more strongly affected than others (Tahara & Larsson, 2013; Buytaert et al., 2014). Studies report shrinkage ranging from extreme (Vickerton et al., 2013; Buytaert et al., 2014), to intermediate (Degenhardt et al., 2010; Düring et al., 2013; Tahara & Larsson, 2013; Li et al., 2016), to absent (Gignac & Kley, 2014; Hughes et al., 2016), with a positive correlation between levels of shrinkage and increasing I2KI concentration (Degenhardt et al., 2010). The majority of specimens subjected to diceCT thus far have been fresh field-collected specimens rather than preserved museum specimens (but see Herdina et al., 2010; Cox & Jeffery, 2011; Jeffery et al., 2011; Cox & Faulkes, 2014; Herdina et al., 2015a, 2015b). The utility of I₂KI staining, and its impact on the shrinkage of soft-tissues, in museum specimens has not yet been assessed systematically. Knowledge regarding the suitability, and limitations, of including museum specimens in soft-tissue studies is important as they become increasingly used to broaden taxonomic sampling.

We document the effects of I_2KI -based staining, and the length of time a specimen has been stored in a museum collection, on potential shrinkage in soft-tissues. We quantified the relative volume of brain and eye tissue in five specimens of whole bats collected between 20 and 110 years ago at four time points during the staining process (1, 2, 3, and 4 weeks in I_2KI). These data allowed us to address three questions. First, how long should small museum specimens be stained with I_2KI in order to optimize contrast? Second, how does the length of exposure to I_2KI affect the volume of soft-tissues in museum specimens? Third, is the length of time since specimen collection associated with the relative volumes of brain and eye tissue? By addressing these questions, we aim to provide technical guidance to researchers planning to use diceCT to quantify and compare the volume of soft-tissues in museum specimens.

In certain cases (e.g., studies concerning rare or protected species, or those with limited museum collections), it may be necessary to combine soft-tissue measurements from freshly collected specimens (not fixed in ethanol) and museum specimens into one data set. Therefore, in order to assess how these different tissues react to I₂KI staining, we took the opportunity to compare relative tissue size in our five museum specimens to that of six bat specimens that were all stained and imaged within 1 year after collection. Using these specimens we asked, how do museum specimens compare with recently collected field specimens in terms of potential shrinkage? The field-collected specimens were not preserved and stained in exactly the same way as the museum specimens were, which is often the case in genuine comparative studies, however, differences between them do suggest variables that may play a role in the relative volume reduction of soft-tissues in museum specimens.

Materials and Methods

Specimens

We carried out contrast-enhanced μ CT by submerging five bats from the American Museum of Natural History Collection (AMNH) and six bats collected from Peru and the Dominican Republic in a solution of Lugol's iodine (I2KI). For purposes of reference in this study, we define specimens from the AMNH collection as the "museum sample" given their long residency in museums and bats collected from Peru and the Dominican Republic as the "field sample" given their recent acquisition from the field and lack of exposure to ethanol. The museum sample consisted of bats from the superfamily Noctilionoidea and exhibited a range of body masses: Glossophaga soricina (9.6 g), Carollia perspicillata (18 g), Desmodus rotundus (25-40 g), Artibeus jamaicensis (38-48 g), and Artibeus lituratus (65.9 g) (Greenhall et al., 1983; Alvarez et al., 1991; Cloutier & Thomas, 1992; Stockwell, 2001; Ortega & Castro-Arellano, 2001). These bats were in museum collections for varying periods of time, having been collected from between 1907 and 1993. As is the case for the vast majority of museum specimens, there was no information describing how they were originally prepared and fixed for storage. This is commonly the case in museum collections and was therefore, unavoidable. However, we do know they had all been stored for long periods of time in 70% ethanol.

The field-collected bats were obtained from two field sites in Peru (Faique, San Cristábol and Jenaro Herrera, Loreto), and one site in the Dominican Republic (Jaragua) (IACUC protocols 614763-2 and 554555-3 issued by Stony Brook University). Specimens were sacrificed using isofluorane and then immediately placed in 10% phosphate-buffered formalin. Specimens remained in formalin for ~10 months until they were transferred to iodine. Only two of the field-collected bats were the same species as the museum specimens, but the range of body masses of the two data sets was similar (museum sample: 9.6-65.9 g; field sample: 7-27 g). Five species of this data set are noctilionoids: Rhinophylla pumilo (7–14 g), G. soricina (9.7 g), Anoura geoffroyi (10-15 g), Phyllops falcatus (16-23 g), and C. perspicillata (17 g), with one additional species from the closely related family Molossidae, Molossus molossus (21-27 g) (Alvarez et al., 1991; Cloutier & Thomas, 1992; Jennings et al., 2000; Rinehart & Kunz, 2006; Da Cunha Tavares & Mancina, 2008; Ortega & Alarcón-D, 2008). The Peru specimens are on loan and will be returned to the Colección CEBIO in Lima, Peru upon completion of this study. The Dominican Republic samples are part of the collections at the Dávalos lab at Stony Brook University.

Sample Preparation, Scanning, and Reconstruction

Before staining in I_2KI , the museum specimens were scanned to optimize bone contrast using the Nikon Metrology (X-Tek) HMXST225 (Nikon Metrology Inc., Tokyo, Japan) MicroCT system at the Center for Nanoscale Systems at Harvard University. This scanner has a peak voltage of 225 kV and all scans were done using a molybdenum target. Given that I_2KI and other contrast agents increase the X-ray attenuation of soft-tissue so that it is similar to bone, it is recommended to scan specimens optimizing for bone before performing iodine staining if hard tissue data are also needed (Düring et al., 2013; Gignac et al., 2016). It is possible to segment out bone manually after staining with I_2KI (Baverstock et al., 2013), but this takes more time. Field-collected specimens were not scanned to optimize for bone before staining with I_2KI stain and so

bone was manually segmented from the I₂KI-stained scans. Scan parameters and voxel size for each hard tissue optimized scan are shown in Supplementary Table A1.

After taking scans optimized for hard tissue, we put each museum specimen in 10% phosphate-buffered formalin (4% formaldehyde) for 12 days before staining with I₂KI to reduce potential shrinkage, as recommended in previous studies (Baverstock et al., 2013; Gignac & Kley, 2014; Gignac et al., 2016). Each museum specimen was then placed into a 2.5 w/v% solution of I2KI and scanned at weekly intervals for 4 weeks. One week was set as the lower limit because pilot scans suggested that contrast was poor in specimens stained for short periods of time. We decided upon 2.5 w/v% I₂KI, given that previous studies effectively visualized similarly sized specimens using 3.25-3.75 w/v% I2KI (Jeffery et al., 2011; Baverstock et al., 2013; Tahara & Larsson, 2013). Specimens were stained whole to both preserve their integrity and reduce the possibility of shrinkage, based on the suggestion that staining entire specimens is effective in such a reduction (Tahara & Larsson, 2013). The I₂KI solution was not refreshed during the staining process given that the solution did not lighten in color across the 4-week interval for any specimens. The specimens were taken out of solution only for the duration of the scans and were placed in sealed bags during scans to reduce desiccation.

Specimens collected in the field were stained for 15-18 weeks. Although it would have been ideal to stain them for the same amount of time as the museum specimens, this was not possible due to logistic reasons. Therefore, this provides a conservative estimate of the effects of museum collection and storage procedures on shrinkage in soft-tissues. If I₂KI staining causes substantial shrinkage over time (e.g., Vickerton et al., 2013), then the field-collected specimens should exhibit more shrinkage than any of the museum specimens. If the field-collected specimens exhibit less shrinkage despite being stained for a longer period of time, then one or more aspects of the preparation and storage has a more substantial effect on shrinkage. As the staining time differed between museum and field specimens, and preservation and storage procedures for museums specimens were unknown, a formal test of which factors caused potential differences between the two data sets is beyond the scope of our study.

Scans were aligned using proprietary software associated with the X-Tek CT scanner (CTPro; Nikon Metrology Inc., Tokyo, Japan) and then reconstructed in VGStudio Max 3.0 (Volume Graphics Inc., Germany), such that the contrast between tissues was optimized for each specimen individually. Image stacks were then exported and uploaded into Mimics v. 16.0 (Materialise, Leuven, Belgium) for 3D segmentation. Although it is possible to automate segmentation in Mimics, the contrast of tissues stained with I₂KI is generally similar and manual segmentation is often preferred (Cox & Jeffery, 2011; Aslanidi et al., 2013; Baverstock et al., 2013). Previous studies have demonstrated that inter-operator variability and bias is low in manually segmented scans (Buytaert et al., 2014). The majority of scans were segmented by B.P.H. and for those that were not, each individual slice was checked manually by B.P.H. to ensure low inter-operator variability.

Brains and eyes were chosen for assessing relative volume changes because they can be confidently segmented and visualized, and are often the subjects of comparative and anatomical research (e.g., Hautier et al., 2012; Girard et al., 2016; Gold et al., 2016; Hughes et al., 2016). After segmentation, brain and eye models were smoothed to reduce surface noise and exported as STL files into Geomagic Studio 2014 (3DSystems, SC, USA).

For brains, data from all 4 weeks of a particular specimen were aligned using the Geomagic best-fit alignment function and were sectioned at the same point on the brainstem so as to include the same proportion of brainstem volume in each model. Both eyes were segmented and then averaged to generate a mean eye volume for each specimen. In general, both eyes in the same specimen were similar in volume. Brain and eye volumes were calculated from STLs in Geomagic (Supplementary Table A2).

In order to estimate the original size of the brains and eyes, the endocranial volume and volume of the orbital space were used as proxies. Endocranial volume was calculated using the 3D skull models generated from scans that were optimized for bone (museum specimens), and scans for which bone was segmented manually in Mimics (field-collected specimens). All eyes, including those of field-collected specimens, were surrounded by a black space in CT scans. We manually segmented that space in Mimics and used it as a proxy for orbital volume. Muscle tissues define the orbital space and so it too may have incurred some volume reduction resulting from shrinkage. Further, differences in the orbital contents between species such as the relative size of extraocular muscles and the presence of glands or fat bodies may have generated relatively larger orbital spaces in some species than others (Rehorek et al., 2010). However, there was much less substantial muscular volume reduction noted in comparison with eyes, and thus we consider it the best proxy available. As with the eyes, the right and left orbital spaces were segmented separately and averaged to generate an average volume for each specimen. Models of the orbital space and endocranium were then exported as STLs and their volumes were measured in Geomagic (Supplementary Table A2).

We defined eye shrinkage as the relative difference between the volumes of the globe and orbital space, and brain shrinkage as the relative difference between the volumes of the brain and endocranial space. The endocranial cavity houses the brain as well as cranial nerves, vessels, and periorbital fat. Differential allometry of these accessory tissues could be an issue if the sample contained species of very different sizes. However, this is not the case for our sample, which contained only bats that ranged from 10 to 65 g in body mass.

A primary goal of our study was to determine the optimum stain time to generate a high contrast scan useful for segmenting soft-tissue structures in bat-sized vertebrates. Although noctilionoid bats are quite small, previous studies have found that somewhat larger taxa (e.g., Sciurus carolinensis; 338-750 g; Ruff & Wilson, 1999) required very long stain times of around 7 weeks at higher stain concentrations than we used (20 w/v% I₂KI) for iodine to completely penetrate deeper tissues (Jeffery et al., 2011). A number of studies have quantified differences between different stain methods, or tested a single stain method across a time series by calculating differences in contrast between different parts of a scan or between a scanned region and a standard (Pauwels et al., 2013; Gignac & Kley, 2014; Girard et al., 2016; Li et al., 2016). Since we were only interested in visualizing the soft-tissue structures well enough to segment them for morphometric analyses, we used a qualitative approach of visually comparing week-by-week scans similar to that used by Descamps et al. (2014).

Statistical Analyses

To ensure that volume data were collected with limited error and maximum precision, B.P.H. measured the left and right eyes and orbital spaces of AMNH 249088 (week 2) four times on separate

days to create a replicate data set. Eye volume for the replicate data set ranged from 1.44 to 1.56 mm³ and orbital space volume ranged from 3.20 to 3.75 mm³. To assess error, we calculated the standard deviation for the replicate data set and compared it to the standard deviations for each museum specimen for weeks 1 through 4. We then took the mean of the standard deviation for all weeks of all five museum specimens and compared that to the standard deviation for the replicates to see if the standard deviation of the sensitivity data set was substantially less than that of the replicates.

Volume measurements were imported into R for statistical analysis (R Core Development Team, 2016). To test whether tissues from museum specimens reduced in volume as a result of time in I₂KI, we ran ordinary least squares regressions of brain and eye volume against time in stain with volume as the dependent variable and number of weeks in stain as the independent variable at a significance level of $\alpha = 0.05$. Previous studies found that soft-tissue shrank exponentially and not linearly in response to I₂KI (Vickerton et al., 2013). However, a linear model was the best fit for our data and so we used the linear model function in the stats package in R. To test if time since collection affected volume reduction, we regressed the brain-endocranial ratio and eye-orbital space ratio against time since museum specimens were collected using repeated measures analysis of variances with a significance level of $\alpha = 0.05$. We quantified the extent to which museum specimens exhibited greater volume reduction in comparison with field-collected specimens by comparing ratios of brain volume to endocranium volume and eye volume to orbital space volume using a two-sample t-test in the stats package in R.

Results

Qualitatively, the ability to differentiate tissues was similar for all museum specimens from weeks 1 to 4 with limited improvement over time. It was easy to visualize eyes and brains for all specimens for all 4 weeks (Fig. 1). As in other studies the eye lenses were intensely stained (Metscher, 2009a). Therefore, it is possible to stain noctilionoid-sized animals for 7 days using an $\rm I_2KI$ concentration of 2.5 w/v% and expect acceptable contrast between tissues and complete penetration of the stain deep into the skulls. Further, 4 weeks in an unrefreshed 2.5 w/v $\rm I_2KI$ solution did not lead to oversaturation of soft-tissue for noctilionoid-sized taxa.

The sensitivity analysis using AMNH 249088 (week 2) replicates showed that the mean of our standard deviations for all weeks

and all bats was larger than that of the replicate data set for both the eyes ($SD_{replicate} = 0.053$, $SD_{all} = 0.085$) and the orbits ($SD_{replicate} = 0.073$, $SD_{all} = 0.191$) (Supplementary Figs. A1a and A2a). However, for certain bats, the standard deviation of weeks 1–4 was similar to, or even less than, the standard deviation of the replicate data sets for both the eyes and orbits (Supplementary Figs. A1b and A2b). This indicates negligible changes in volume from week to week that, in some cases, were indistinguishable from measurement error. Although each museum-based species had relative decreases in brain volume from weeks 1 to 4, the only significant trend was found in *A. jamaicensis* (F(1,2) = 39.69, p = 0.024, Fig. 2). Similarly, eye volume generally decreased in all museum specimens from week to week, though only significantly for *A. lituratus* (F(1,2) = 73.9, p = 0.013, Fig. 3).

When comparing relative brain and eye volumes between museum-based specimens and field-collected specimens, we found a significant difference in means (Table 1). The mean brain–endocranial ratio for museum-based specimens was 0.62 (SD=0.092), suggesting a volume reduction of 38%. In contrast, the average brain–endocranial ratio of field-collected specimens was 0.94 (SD=0.016), suggesting a volume reduction of only 6% (Fig. 4). The mean eye–orbital space ratio for museum specimens was 0.57 (SD=0.056, suggesting a volume reduction of 43%), while the mean ratio for field-collected specimens was 0.74 (SD=0.073, suggesting a volume reduction of 26%). The eyes exhibited substantially larger relative differences in volume than brains in field-specimens, while the standard deviations of the ratios for the eyes and brains of museum specimens overlapped (Fig. 4).

To evaluate whether the amount of time specimens spent in museum collections influenced these volume differences, we regressed the brain–endocranial ratio and eye–orbital space ratios against years the specimens were collected. We found no significant trends for either relative brain volume (F(1,18) = 0.007, p = 0.94) or eye volume (F(1,18) = 0.019, p = 0.898) based on time since specimens were collected (Fig. 5). The specimens most different from one another were collected only a year apart, in 1978 and 1979, underscoring the lack of pattern in the data.

Discussion

In order to conduct broad comparative analyses, morphologists often turn to existing museum specimens because it is usually impractical to collect large numbers of different species in the field specifically for a single study. However, it is currently unclear

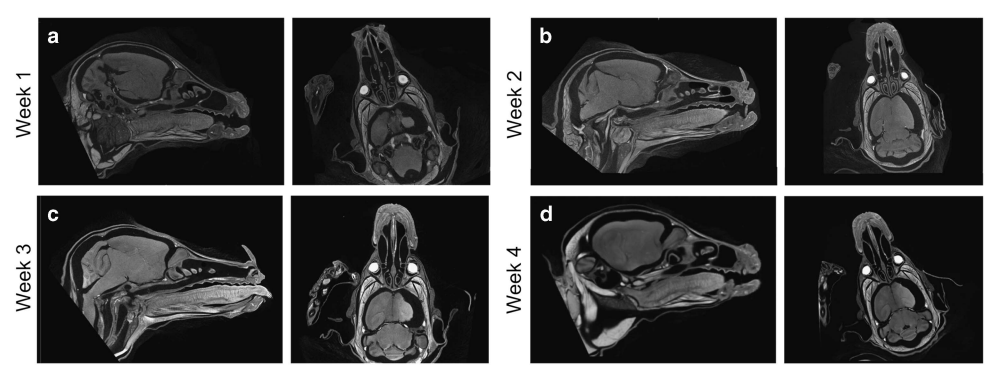


Figure 1. Weeks 1–4 mid-sagittal and mid-transverse slices showing relative iodine-based solution (I₂KI) penetration and differentiation of tissues (*Glossophaga soricina* (AMNH 239885)). From week to week, there is minimal qualitative improvement in tissue contrast suggesting that for noctilionoid-sized bats, 1–2 weeks of stain time is sufficient using a 2.5 w/v% concentration of I₂KI.

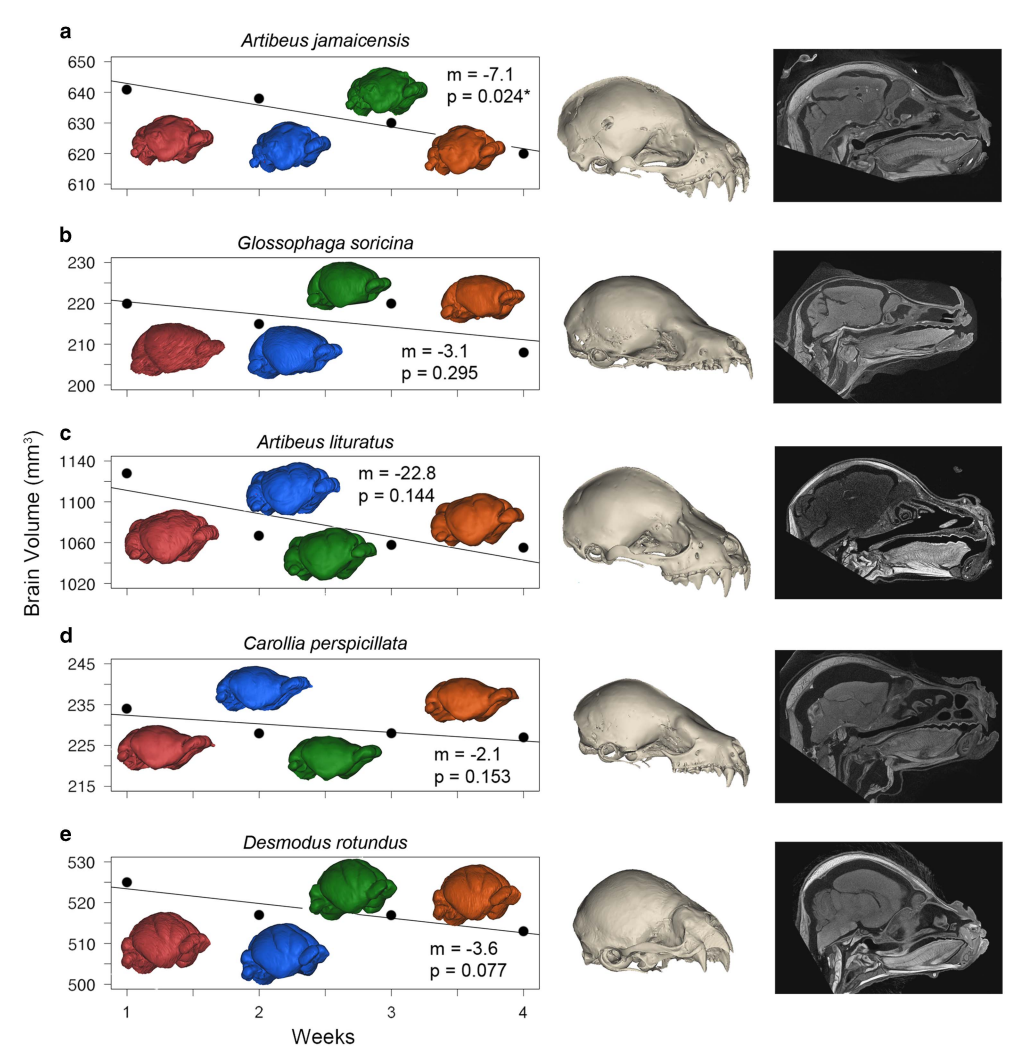


Figure 2. Ordinary least squares regression for time in stain (in weeks) by brain volume (mm³) with associated three-dimensional reconstructed skull and sample mid-sagittal slice of the soft-tissue. **a:** *Artibeus jamaicensis* (AMNH 69111). **b:** *Glossophaga soricina* (AMNH 239885). **c:** *Artibeus lituratus* (AMNH 237919). **d:** *Carollia perspicillata* (AMNH 249088). **e:** *Desmodus rotundus* (AMNH 267652). Only the brain of *A. jamaicensis* decreases significantly in volume week to week suggesting minimal impact of iodine-based solution (I₂KI) stain time on shrinkage. m is the slope. * indicates significance. Week 1: red; week 2: blue; week 3: green; week 4: orange.

how useful these fixed museum specimens are for studies of softtissues using methods such as diceCT. In this study we found that neither the length of time that museum specimens are immersed in stain (Figs. 2, 3) or have been stored in a museum collection (Fig. 5) has a significant effect on volume of the brain and eye relative to the proxies of initial brain and eye size. Nevertheless, the volumes of the eyes and brains of the museum specimens were, on average, only 57 and 62% of our estimates of their original sizes (volume reductions of 43 and 38%, respectively), while the eyes and brains of field-collected specimens exhibited significantly smaller changes in volume, at 74 and 94% of the size of the proxies of original volume (volume reductions of 26 and 6%, respectively) (Fig. 4). Although this study does not reveal the cause of this difference, variables associated with fixation, initial steps in specimen preparation, and field conditions are reasonable candidates.

Shrinkage to this extent has not been reported in other studies when low concentrations of I_2KI were used (but see Buytaert et al., 2014), likely because the majority of previous studies have used relatively fresh specimens. The field-collected specimens in this study did exhibit some relative size reduction, but they retained more of their original volume, based on proxies of

original size, than the museum specimens and were similar to levels of shrinkage reported in previous studies. However, it is important to note that methods for calculating shrinkage vary between studies.

Vickerton et al. (2013) found extreme shrinkage in freshly collected skeletal muscle, cardiac muscle, and the cerebellum of mice when stained using 2, 6, 10, and 20 $\text{ w/v}\% \text{ I}_2\text{KI}$, with 2 $\text{ w/v}\% \text{ I}_2\text{KI}$ resulting in mouse hearts that shrunk 20%.

This shrinkage was shown to be much larger than the effect of formalin fixation alone, which was estimated to cause 12% shrinkage. Vickerton et al.'s (2013) 2 w/v% I₂KI results compare well to the shrinkage found in our field-collected eyes, which reduced in size 26% (Fig. 4). Other studies have found much less shrinkage than Vickerton et al. (2013) (ranging from 4.4 to 10% shrinkage) (Schmidt et al., 2010; Tahara & Larsson 2013; Li et al., 2016). The results of these studies are similar to the field-collected brains in this study, which showed a 6% reduction in size relative to our proxies of original size (Fig. 4). Eyes seem to be particularly susceptible to shrinkage, likely because they are largely fluid-filled. Both tissue type and stain concentration appear to be factors affecting shrinkage, leading to the variation in shrinkage reported in previous studies. By contrast, the museum specimens in this

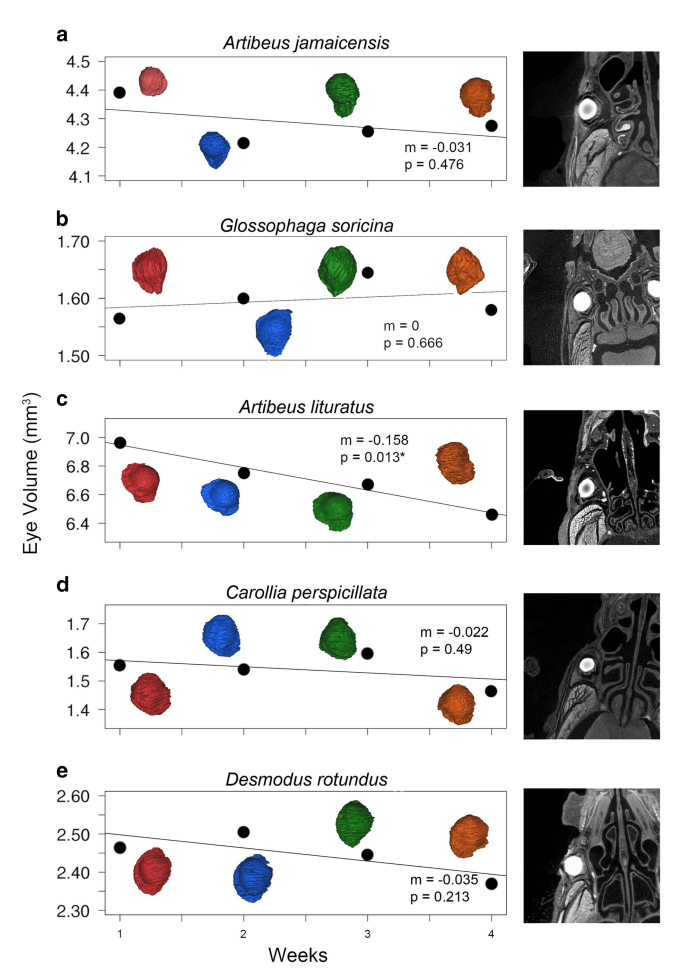


Figure 3. Ordinary least squares regression for time in stain (in weeks) by eye volume (mm³) with associated transverse slice through the eye. **a:** *Artibeus jamaicensis* (AMNH 69111). **b:** *Glossophaga soricina* (AMNH 239885). **c:** *Artibeus lituratus* (AMNH 237919). **d:** *Carollia perspicillata* (AMNH 249088). **e:** *Desmodus rotundus* (AMNH 267652). Eye volume is averaged across both eyes. Similar to brain volume, only one bat shows statistically significant shrinkage week to week (*A. lituratus*). m is the slope. * indicates significance. Week 1: red; week 2: blue; week 3: green; week 4: orange.

study had an average size reduction of 38% in the brains and 43% in the eyes relative to proxies of original size. Buytaert et al. (2014) similarly found large amounts of shrinkage in brain tissue (27–66% shrinkage) using 3 w/v% I_2KI . It is possible that the high magnitudes of shrinkage in the relatively fresh specimens studied by Buytaert et al. (2014) were caused by the tissues being studied as blocks rather than as whole, intact specimens. Tissue blocks have been shown to be much more susceptible to shrinkage than intact specimens (Fox et al., 1985).

Table 1. Differences Between Museum-Based and Field-Collected Specimens.

	<i>t</i> -Statistic	p Value	Museum- Specimen Average	Field- Specimen Average
Eye-orbital space ratio	-5.8453	<0.001	0.57 (±0.056)	0.74 (±0.073)
Brain-endocranial space ratio	-14.548	<0.001	0.62 (±0.092)	0.94 (±0.016)

The museum specimens have significantly more shrinkage in both their eye-orbital space ratio and in their brain-endocranial ratio in comparison with field-collected specimens based on a two-sample *t*-test. Note the large differences in means between groups. Standard deviations in parentheses.

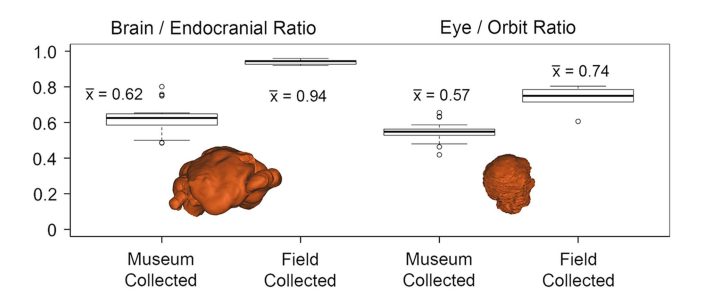


Figure 4. Box plots for museum-based and field-based brain–endocranial ratios and eyeorbital space ratios with associated means. Graphical demonstration of the significantly higher volume reduction associated with the museum-based specimens than the fieldcollected specimens for both the eye and brain. Example brain and eye inset.

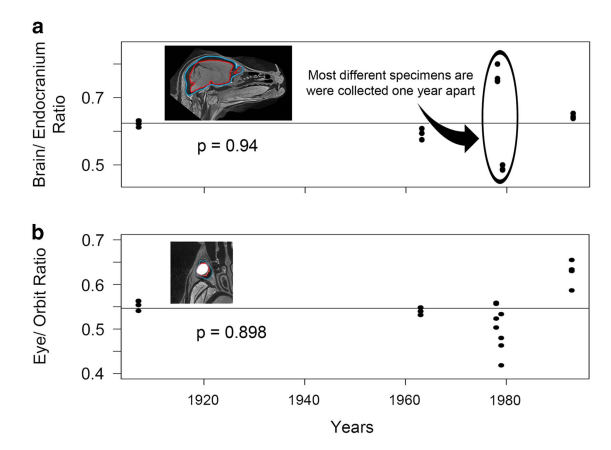


Figure 5. Repeated measures regressions showing museum-based specimen brainendocranial ratios (a) and eye-orbital space ratios (b) as a function of time since specimens were collected. The relationship between time since collection and both brain and eye shrinkage were not significant suggesting that time since specimens were placed in collections was not important to the amount of volume reduction observed. This is supported by the fact that the largest amount of variance is found between the specimens collected in 1978 and 1979. All four weeks for the stain-time sensitivity analysis were included to account for within-specimen variance in volume reduction.

In the absence of other explanations, fixation is commonly viewed as the primary culprit causing shrinkage. Formalin fixation is a necessary step in the diceCT process because it stabilizes the tissue before submersion and reduces shrinkage caused by I2KI (Gignac et al., 2016). Moreover, formalin is preferred to fixatives such as ethanol because it does not reduce the effectiveness of iodine staining. It is also a standard step when preparing specimens in the field, although it was not widely performed until the late 1800s (Fox et al., 1985). Formaldehyde is an excellent fixative because it is effective over a large range of concentrations and can be used for a wide variety of tissues. However, fixation in formalin has long been recognized to cause some degree of shrinkage based on studies involving tissue blocks (Ericsson & Biberfeld, 1967; Dam, 1979) with more recent studies finding limited shrinkage caused by formalin fixation (1-5%) in concentrations lower than 40% (Fox et al., 1985; Baverstock et al., 2013; Düring et al., 2013; Hughes et al., 2016). This shrinkage range is comparable to what we found in field-collected brains, suggesting that I₂KI may not have had a shrinkage effect beyond the shrinkage caused by formalin. However, formalin fixation does not explain the extreme size reduction in the soft-tissues of our museum specimens.

Exposure to ethanol is the most striking difference between the museum- and field-collected specimens in the way that they were processed and stored. The field-collected specimens went straight from formalin to $\rm I_2KI$ and were never subjected to ethanol while museum specimens were stored in 70% ethanol for many years.

Ethanol penetrates specimens and dehydrates them, which helps to preserve them (Sturgess & Nicola, 1975). However, this also has a known shrinkage effect (Vervust et al., 2009). Our study focused on the effects of I₂KI and long-term storage on the volume of soft-tissues in museum specimens, but did not directly examine the effect of ethanol on specimen shrinkage when examined with diceCT. Future experiments comparing soft-tissues in specimens that are fixed with formalin and stored for different lengths of time and in different concentrations of ethanol would help to pinpoint the effects of ethanol on museum specimens, and may help generate improvements for field-collection methodology (see Hughes et al., 2016).

Variation in field preparation techniques and conditions could also differentially affect shrinkage of soft-tissues in museum specimens. It is unusual to know the concentrations, exposure time, or even the fixatives that were used to prepare specimens in the field. The challenges of fieldwork sometimes require creative solutions. For example, rum is sometimes used as a fixative when ethanol and/or formalin are not available. Low temperatures can also cause increased shrinkage in formaldehyde-fixed specimens (Fox et al., 1985). These factors may explain the different degree of shrinkage in the brains and eyes of our specimens collected in 1978 and 1979 (Fig. 5). Recent work by Hughes et al. (2016) examined the effectiveness of several field preservation techniques in harsh field conditions. The team identified three techniques for preserving field specimens for immunohistochemistry and imaging with diceCT that yielded tissues equal in quality to those prepared in the lab. Although this study did not address the long-term storage needs of museums directly, the results are encouraging and we hope that the field techniques gain purchase in the collections community.

Overall, we emphasize that relatively fresh field-collected tissue is optimal when shrinkage is a concern, but note that it can be difficult to obtain in comparison with museum specimens. Our study provides an invaluable assessment of methodological artifacts and provides a starting point for future studies seeking to incorporate museum specimens in vertebrate soft-tissue comparative analyses, as diceCT continues to emerge as a primary tool for such studies. Given the overlap in confidence intervals of the brain/endocranial ratio and the eye/orbital space ratio (Fig. 4), it is possible that a realistic generalized correction factor for museum specimen softtissue may be obtainable. However, the large variation between the specimens from 1978 and 1979 demonstrates that more museum specimens need to be evaluated using diceCT before an accurate correction factor can be proposed. It is possible that these two specimens are aberrant and had unusual field preservation methods (e.g., fixation in rum), but it is also possible that variation in museum specimen soft-tissue shrinkage is truly large and that these specimens are not outliers. Nearly all comparative morphologists require museum specimens in order to visualize, quantify, and compare soft-tissues when seeking to examine evolutionary trends and therefore this work will be paramount to the successful melding of diceCT with museum specimens in volumetric comparative studies. As such, our identification of the complexity of this issue is an important first step to the development of a correction factor.

Conclusions

DiceCT is a powerful method for examining soft-tissue structures quickly and non-destructively (Gignac et al., 2016). Although the application of diceCT to museum specimens for examining soft-tissue structures at high resolution is a tantalizing prospect, especially when broad phylogenetic representation is needed, we emphasize the need for caution in interpreting results of analyses that compare soft-tissue

volumes using museum specimens until we better understand shrinkage in museum specimens. We found shrinkage in this sample of bat brains to be 32% greater in museum specimens than relatively fresh, field-collected specimens, and shrinkage was 17% greater in their eyes. The differential shrinkage among tissues, with eyes being more strongly affected than brains suggests that studies looking across different tissue types should also use caution when interpreting results. The causes underlying intense shrinkage in museum specimens remains unclear and future work using a larger sample size is needed to uncover the cause or causes. Ethanol is a likely culprit and other potential factors include temperature of specimen storage, the concentration of fixative, and time left in the fixative. We show that one to four weeks of iodine staining and time in museum collections do not correlate with the degree of shrinkage seen in our museum specimens. Future studies should also focus efforts on developing corrections for said shrinkage, either holistically or more likely, for different tissue types. More museum-based diceCT data will be critical in clarifying the causes of shrinkage allowing morphological data from museum specimens generated using diceCT to be appropriately analyzed and corrected for shrinkage.

Supplementary materials. To view supplementary material for this article, please visit https://doi.org/10.1017/S1431927618000399

Acknowledgments. The authors would like to thank Gregory Lin (Harvard University) and Jim Reynolds (Harvard University) for access to the μ CT scanner used in this study as well as technical support. This work was performed in part at the Center for Nanoscale Systems (CNS), a member of the National Nanotechnology Coordinated Infrastructure Network (NNCI), which is supported by the National Science Foundation under NSF award no. 1541959. CNS is part of Harvard University. The authors would like to thank Dan Pulaski (UMass Amherst) for technical support. The authors would like to thank Paul Gignac (Oklahoma State University) and Nancy Simmons (AMNH) for discussions on iodine protocol and the issue of shrinkage. The authors would also like to thank Nancy Simmons, Eleanor Hoeger, and Brian O'Toole (AMNH) for access to museum specimens. Finally, The authors would like to thank our undergraduates for help segmenting eyes and brains, specifically Mateo Frare, Christian Lanzing, Danny Tran, and Chandler Kupris (UMass Amherst). The authors would like to thank Edward Vicenzi and two anonymous reviewers for comments that greatly improved the quality of this manuscript. Research was conducted under NSF-DEB 1442142, 1442278, and 1442314.

References

Alvarez J, Willig MR, Jones JK and Webster WD (1991) Glossophaga soricina. Mamm Species 379, 1–7.

Aslanidi OV, Colman MA, Zhao J, Smaill BH, Gilbert SH, Hancox JC, Boyett MR and Zhang H (2012) Arrhythmogenic substrate for atrial fibrillation: Insights from an integrative computation model of pulmonary veins. 34th Ann Int Conf IEEE EMBS 28, 203–206.

Aslanidi OV, Nikolaidou T, Zhao J, Smaill BH, Gilbert SH, Holden AV, Lowe T, Withers PJ, Stephenson RS, Jarvis JC, Hancox JC, Boyett MR and Zhang H (2013) Application of micro-computed tomography with iodine staining to cardiac imaging, segmentation, and computational model development. *IEEE Trans Med Imaging* 32, 8–17.

Baverstock H, Jeffery NS and Cobb SN (2013) The morphology of the mouse masticatory musculature. *J Anat* 223, 46–60.

Buytaert J, Goyens J, de Greef D, Aerts P and Dirckx J (2014) Volume shrinkage of bone, brain and muscle tissue in sample preparation for micro-CT and light sheet fluorescence microscopy (LSFM). Microsc Microanal 20, 1208–1217.

Chandler N, Aslanidi O, Buckley D, Inada S, Birchall S, Atkinson A, Kirk D, Monfredi O, Molenaar P, Anderson R, Shama V, Sigg D, Zhang H, Boyett M and Dobrzynski H (2011) Computer three-dimensional anatomical reconstruction of the human sinus node and a novel paranodal area. *Anat Rec* 294, 970–979.

- Cloutier D and Thomas DW (1992) Carollia perspicillata. Mamm Species 417, 1–9.
 Cox PG and Faulkes CG (2014) Digital dissection of the masticatory muscles of the naked mole-rat, Heterocephalus glaber (Mammalia, Rodentia). Peer J
 2 e448
- Cox PG and Jeffery NS (2011) Reviewing the morphology of the jaw-closing musculature in squirrels, rats, and guinea pigs with contrast-enhanced microCT. Anat Rec 294, 915–928.
- Da Cunha Tavares V and Mancina CA (2008) *Phyllops falcatus* (Chiroptera: Phyllostomidae). *Mamm Species* 811, 1–7.
- Dam AN (1979) Shrinkage of the brain during histological procedures with fixation in formaldehyde solutions of different concentrations. *J Hirnforsch* 20, 115–119.
- Degenhardt K, Wright AC, Horng D, Padmanabhan A and Epstein JA (2010) Rapid 3D phenotyping of cardiovascular development in mouse embryos by microCT with iodine staining. *Circ Cardiovasc Imaging* 3, 314–322.
- Descamps E, Sochacka A, de Kegel B, Van Loo D, Van Hoorebeke L and Adriaens D (2014) Soft-tissue discrimination with contrast agents using micro-CT scanning. *Belg J Zool* 144, 20–40.
- Düring DN, Ziegler A, Thompson CK, Ziegler A, Faber C, Müller J, Scharff C and Elemans CPH (2013) The songbird syrinx morphome: A three-dimensional, high-resolution, interactive morphological map of the zebra finch vocal organ. BMC Biol 11, 1–27.
- Ericsson JLE and Biberfeld P (1967) Studies on aldehyde fixation. Lab Invest 17, 281.
- Fox CH, Johnson FB, Whiting J and Roller PP (1985) Formaldehyde fixation. J Histochem Cytochem 33, 845–853.
- George ID and Holliday CM (2013) Trigeminal nerve morphology in Alligator mississippiensis and its significance for crocodyliform facial sensation and evolution. Anat Rec 296, 670–680.
- Gignac PM and Kley NJ (2014) Iodine-enhanced microCT imaging: Methodological refinements for the study of the soft-tissue anatomy of post-embryonic vertebrates. J Exp Zool 322B, 166–176.
- Gignac PM, Kley NJ, Clarke JA, Colbert MW, Morhardt AC, Cerio D, Cost IN, Cox PG, Daza JD, Early CM, Echols S, Henkelman RM, Herdina AN, Holliday CM, Li Z, Mahlow K, Merchant S, Müller J, Orsbon CP, Paluh DJ, Thies ML, Tsai HP and Witmer LM (2016) Diffusible iodine-based contrast-enhanced computed tomography (diceCT): An emerging tool for rapid, high-resolution, 3-D imaging of metazoan soft tissues. J Anat 228, 889–909.
- Girard R, Zeineddine HA, Orsbon C, Tan H, Moore T, Hobson N, Shenkar R, Lightle R, Shi C, Fam MD, Cao Y, Shen L, Neander AI, Rorrer A, Gallione C, Tang AT, Kahn ML, Marchuk DA, Luo Z and Awad IA (2016) Micro-computed tomography in murine models of cerebral cavernous malformations as a paradigm for brain disease. *J Neurosci Methods* 271, 14–24.
- Gold MEL, Schulz D, Budassi M, Gignac PM, Vaska P and Norell MA (2016) Flying starlings, PET, and the evolution of volant dinosaurs. Curr Biol 26, R265–R267.
- Greenhall AM, Joermann G and Schmidt U (1983) Desmodus rotundus. Mamm Species 202, 1-6.
- Hautier L, Lebrun R and Cox PG (2012) Patterns of covariation in the masticatory apparatus of hystricognathous rodents: Implications for evolution and diversification. J Morphol 273, 1319–1337.
- Herdina AN, Herzig-Straschil B, Hilgers H, Metscher BD and Plenk H (2010) Histomorphology of the penis bone (baculum) in the Gray Long-Eared Bat Plecotus austriacus (Chiroptera, Vespertilionidae). Anat Rec 293, 1248–1258.
- Herdina AN, Kelly DA, Jahelková H, Lina PHC, Horáček I and Metscher BD (2015a) Testing hypotheses of bat baculum function with 3D models derived from microCT. J Anat 3, 229–235.
- Herdina AN, Plenk H, Benda P, Lina PHC, Herzig-Straschil B, Hilgers H and Metscher BD (2015b) Correlative 3D-imaging of *Pipistrellus* penis micromorphology: Validating quantitative microCT images with undecalcified serial ground section histomorphology. *J Morphol* 276, 695–706.
- Hughes DF, Walker EM, Gignac PM, Martinez A, Negishi K, Lieb CS, Greenbaum E and Khan AM (2016) Rescuing perishable neuroanatomical information from a threatened biodiversity hotspot: Remote field methods for brain tissue preservation validated by cytoarchitectonic analysis,

- immunohistochemistry, and x-ray microcomputed tomography. *PLoS ONE* 11(5), e0155824.
- Jeffery NS, Stephenson RS, Gallagher JA, Jarvis JC and Cox PG (2011) Micro-computed tomography with iodine staining resolves the arrangement of muscle fibres. J Biomech 44, 189–192.
- Jennings JB, Best TL, Rainey JC and Burnett SE (2000) Molossus pretiosus. Mamm Species 635, 1–3.
- Li Z, Ketchum RA, Yan F, Maisano JA and Clarke JA (2016) Comparison and evaluation of the effectiveness of two approaches of diffusible iodine-based contrast enhanced computed tomography (diceCT) for avian cephalic material. *J Exp Zool* **326B**, 352–362.
- Metscher BD (2009a) MicroCT for comparative morphology: Simple staining methods allow high-contrast 3D imaging of diverse non-mineralized animal tissues. BMC Physiol 9, 1–14.
- Metscher BD (2009b) MicroCT for developmental biology: A versatile tool for high-contrast 3D imaging at histological resolutions. Dev Dyn 238, 632–640.
- Ortega J and Alarcón-D I (2008) Anoura geoffroyi (Chiroptera: Phyllostomidae). Mamm Species 818, 1–7.
- Ortega J and Castro-Arellano I (2001) Artibeus jamaicensis. Mamm Species 662, 1–9.
- Pauwels E, Van Loo D, Cornillie P, Brabant L and Van Hoorebeke L (2013)
 An exploratory study of contrast agents for soft tissue visualization by means of high resolution X-ray computed tomography imaging. *J Microsc* **250**, 21–31.
- R Core Team (2016) R: A language and environment for statistical computing. R Foundation for Statistical Computing, Vienna, Austria. Available at https://www.R-project.org/.
- Rehorek SJ, Smith TD and Bhatnagar KP (2010) The orbitofacial glands of bats: An investigation of the potential correlation of gland structure with social organization. *Anat Rec* 293, 1433–1448.
- Rinehart JB and Kunz TH (2006) Rhinophylla pumilio. Mamm Species 791,
- Ruff S and Wilson D (1999) The Smithsonian Book of North American Mammals. Washington, DC: Smithsonian Institution Press. Pp. 1–750.
- Schmidt E, Parsons T, Jamniczky H, Gitelman J, Trpkov C, Boughner JC, Logan CC, Sensen CW and Hallgrímsson B (2010) Micro-computed tomography-based phenotypic approaches in embryology: Procedural artifacts on assessments of embryonic craniofacial growth and development. BMC Dev Biol 10, 18.
- Shenkar R, Venkatasubramanian PN, Wyrwicz AM, Zhao J, Shi C, Akers A, Marchuk DA and Awad IA (2008) Advanced magnetic resonance imaging of cerebral cavernous malformations: II: Imaging of lesions in murine models. *Neurosurgery* **63**, 790–798.
- Stephenson RS, Boyett MR, Hart G, Nikolaidou T, Cai X, Corno AF, Alphonso N, Jeffery NS and Jarvis JC (2012) Contrast enhanced microcomputed tomography resolves the 3-dimensional morphology of the cardiac conduction system in mammalian hearts. *PLoS ONE* 7(4), e35299.
- Stockwell E (2001) Morphology and flight manoeuvrability in new world leaf-nosed bats (Chiroptera: Phyllostomidae). *J Zool* **254**, 505–514.
- Sturgess JA and Nicola SJ (1975) Preparation of fish for identification and preservation as museum species. The Resources Agency of California, Department of Fish and Game, Inland Fisheries Informational Leaflet 29, Sacramento.
- **Tahara R and Larsson HCE** (2013) Quantitative analysis of microscopic x-ray computed tomography imaging: Japanese quail embryonic soft tissues with iodine staining. *J Anat* **223**, 297–310.
- Tessler M, Barrio A, Borda E, Rood-Goldman R, Hill M and Siddall ME (2016) Description of a soft-bodied invertebrate with microcomputed tomography and revision of the genus *Chtonobdella* (Hirudinea: Haemadipsidae). *Zool Scr* **45**, 552–565.
- **Tsai HP and Holliday CM** (2011) Ontogeny of the alligator cartilago transiliens and its significance for sauropsid jaw muscle evolution. *PLoS ONE* **6**(9), e24935.
- Vervust B, Van Dongen S and Van Damme R (2009) The effect of preservation on lizard morphometrics – An experimental study. Amphib Reptil 30, 321–329.
- Vickerton P, Jarvis JC and Jeffery NS (2013) Concentration-dependent specimen shrinkage in iodine-enhanced microCT. J Anat 223, 185–193.